BRAZILIAN JOURNAL
OF MEDICAL AND BIOLOGICAL RESEARCH
www.bjournal.com.br

ISSN 0100-879X
Volume 45 (3) 179-290 March 2012

BIOMEDICAL SCIENCES
AND
CLINICAL INVESTIGATION

Braz J Med Biol Res, March 2012, Volume 45(3) 273-283

doi: 10.1590/S0100-879X2012007500026

Comparative proteomics analysis of chronic atrophic gastritis: changes of protein expression in chronic atrophic gastritis without Helicobacter pylori infection

Lin Zhang, Yanhong Hou, Kai Wu and Dan Li

Brazilian Journal of Medical and Biological Research (2012) 45: 273-283
ISSN 0100-879X

Comparative proteomics analysis of chronic atrophic gastritis: changes of protein expression in chronic atrophic gastritis without *Helicobacter pylori* infection

Lin Zhang, Yanhong Hou, Kai Wu and Dan Li

Department of Gastroenterology and Hepatology, The 309 Hospital of People's Liberation Army, Beijing, China

Abstract

Chronic atrophic gastritis (CAG) is a very common gastritis and one of the major precursor lesions of gastric cancer, one of the most common cancers worldwide. The molecular mechanism underlying CAG is unclear, but its elucidation is essential for the prevention and early detection of gastric cancer and appropriate intervention. A combination of two-dimensional gel electrophoresis and mass spectrometry was used in the present study to analyze the differentially expressed proteins. Samples from 21 patients (9 females and 12 males; mean age: 61.8 years) were used. We identified 18 differentially expressed proteins in CAG compared with matched normal mucosa. Eight proteins were up-regulated and 10 down-regulated in CAG when compared with the same amounts of proteins in individually matched normal gastric mucosa. Two novel proteins, proteasome activator subunit 1 (PSME1), which was down-regulated in CAG, and ribosomal protein S12 (RPS12), which was up-regulated in CAG, were further investigated. Their expression was validated by Western blot and RT-PCR in 15 CAG samples matched with normal mucosa. The expression level of RPS12 was significantly higher in CAG than in matched normal gastric mucosa ($P < 0.05$). In contrast, the expression level of PSME1 in CAG was significantly lower than in matched normal gastric mucosa ($P < 0.05$). This study clearly demonstrated that there are some changes in protein expression between CAG and normal mucosa. In these changes, down-regulation of PSME1 and up-regulation of RPS12 could be involved in the development of CAG. Thus, the differentially expressed proteins might play important roles in CAG as functional molecules.

Key words: Differentially expressed proteins; Chronic atrophic gastritis; Proteomic study; Ribosomal protein S12 (RPS12); Proteasome activator subunit 1 (PSME1)

Introduction

Chronic atrophic gastritis (CAG) is currently recognized as a special form of chronic gastritis characterized by mucosa atrophy, exposed vessels and mucosal nodules. These features appear to be unusual and different from those seen in other types of chronic gastritis. The diagnosis can be easily made by endoscopic examination and histopathologic evaluation. A number of studies have been conducted to determine the prevalence of CAG in countries having high mortality from gastric cancer, especially in Eastern Asia (1,2). However, recently, the morbidity of CAG has been rapidly increasing in China. The *Helicobacter pylori* bacterium colonizes the stomach mucosa and triggers a series of inflammatory reactions. It is considered to be an important cause of CAG (3,4), as shown in rodent models (5-7). Although a close relationship between this type of gastritis and *H. pylori* has been suggested to exist during the last few years, the role of *H. pylori* still remains unknown. Why are there many CAG patients without *H. pylori* infection? Globally, gastric cancer is the second most common malignancy. Each year, roughly 798,000 people are diagnosed with gastric cancer worldwide (9.9% of total cancer cases) and 628,000 people die from the disease (8). CAG plays a crucial role in the development of the intestinal type gastric cancer and has been considered to be the first step in a sequence of mucosal changes in the stomach leading to cancer. It is widely accepted that gastric carcinogenesis is a continuous process leading from non-atrophic gastritis to CAG (loss of specialized glands), to metaplasia and dysplasia, and finally to adenocarcinoma (9-13). Gastric cancer might be effectively controlled if this premalignant lesion - CAG - is detected and treated before invasion occurs. But the molecular mechanism

Correspondence: Lin Zhang, Department of Gastroenterology and Hepatology, The 309 Hospital of PLA, Beijing 100091, China.
E-mail: stepinghuns2@yahoo.cn

Received July 4, 2011. Accepted February 1, 2012. Available online March 2, 2012. Published March 19, 2012.

underlying this first step leading to gastric cancer is still unknown because molecular biology investigations of CAG are very scarce. Therefore, it is crucial to elucidate the molecular mechanism underlying CAG.

Because the pattern of expressed proteins represents a "library" of information about the functional status and health of the tissue, in recent years, protein extraction, display, and analysis have been developed as new methods representing a new field of clinical proteomics. In this field, the above-mentioned techniques are used to identify functional molecular markers or biomarkers of cancer and other diseases (14), but there are hardly any studies on the differential expression of proteins between CAG and normal-appearing mucosa.

Most current researches focus mainly on the clinical characteristics of this disease, with much less attention paid to molecular changes occurring in the normal-appearing mucosa from which such lesions emerge. In the present study, we used proteomic techniques to test the hypothesis that normal gastric mucosa from a patient with CAG would exhibit patterns of protein expression distinct from the affected mucosa from the same patient. This approach provides a comparison of anatomically normal and disordered tissues against the same genetic background to analyze the molecular mechanism underlying CAG.

Material and Methods

Sample collection

Samples were taken from 21 patients with CAG from the 309 Hospital of the General Hospital of the People's Liberation Army (PLA) (Table 1). Normal gastric mucosa was

Table 1. Characteristics of chronic atrophic gastritis (CAG) patients from whom normal mucosal and CAG lesion biopsies were obtained in the present study.

Patient No.	Gender	Age (years)	Lesion site	Histology
1	F	69	Gastric fundus and antrum	Chronic mucosal inflammation with gastric gland atrophy, HP(-).
2	F	73	Gastric antrum	Acute and chronic mucosal inflammation with gastric gland atrophy, HP(-).
3	F	66	Lower half of gastric body and gastric antrum	Acute and chronic mucosal inflammation with lymphocytic infiltration, HP(-).
4	F	59	Gastric antrum	Acute and chronic mucosal inflammation, HP(-).
5	F	67	Gastric antrum	Acute and chronic mucosal inflammation with gastric gland atrophy, HP(-).
6	F	54	Lower half of gastric body and gastric antrum	Chronic mucosal inflammation with gastric gland atrophy, HP(-).
7	F	58	Gastric antrum	Acute and chronic mucosal inflammation with lymphocytic infiltration, HP(-).
8	F	72	Gastric antrum	Chronic mucosal inflammation with gastric gland atrophy, HP(-).
9	F	65	Lower half of gastric body and gastric antrum	Acute and chronic mucosal inflammation with lymphocytic infiltration, HP(-).
10	M	43	Gastric antrum	Acute and chronic mucosal inflammation with gastric gland atrophy, HP(-).
11	M	52	Gastric antrum and pylorus	Chronic mucosal inflammation, HP(-).
12	M	45	Gastric antrum	Chronic mucosal inflammation with gastric gland atrophy, HP(-).
13	M	65	Lower half of gastric body and gastric antrum	Acute and chronic mucosal inflammation with gland atrophy, HP(-).
14	M	73	Gastric antrum and pylorus	Chronic mucosal inflammation with gland atrophy, HP(-).
15	M	68	Lower half of gastric body and gastric antrum	Acute and chronic mucosal inflammation with gland atrophy, HP(-).
16	M	57	Gastric antrum	Acute and chronic mucosal inflammation, HP(-).
17	M	67	Lower half of gastric body and gastric antrum	Acute and chronic mucosal inflammation with gland atrophy, HP(-).
18	M	74	Gastric antrum	Acute and chronic mucosal inflammation, HP(-).
19	M	43	Gastric antrum	Chronic mucosal inflammation with gastric gland atrophy, HP(-).
20	M	58	Gastric antrum and pylorus	Acute and chronic mucosal inflammation with gland atrophy, HP(-).
21	M	70	Lower half of gastric body and gastric antrum	Chronic mucosal inflammation with gastric gland atrophy, HP(-).

HP = *Helicobacter pylori*.

defined as that 5 cm adjacent to the affected mucosa and with no expression of CAG under endoscopy. All samples were obtained by biopsy in endoscopy examinations of these patients. Four tissue fragments of the CAG focus and of normal mucosa were obtained from each patient. One tissue fragment was used for pathological diagnosis, and the other was saved for future study. The 13C urea breath test was applied to the patients to detect *H. pylori* infection and the results were negative. The results of autoantibody detection were also negative. *H. pylori* infection and autoimmune disease were excluded. The Ethics Committee of Biomedicine of the 309 Hospital of the PLA, China, approved the study and all patients gave written informed consent to participate.

All samples were snap-frozen in liquid nitrogen and stored in a deep freezer (-80°C) until use. Tissues (70-140 mg) were then crushed in liquid nitrogen and lysed in 1 mL 7 M urea, 2 M thiourea, 4% 3-[(3-cholamidopropyl) dimethylammonio] propanesulfonate (CHAPS), 65 mM dithiothreitol (DTT), and 0.2% Bio-Lyte (pH 5-8; Bio-Rad, USA) with sonication on ice. The lysates were centrifuged at 20,000 *g* for 1 h at 4°C, the supernatants were removed and protein concentration was determined with the Bio-Rad AC DC protein assay kit (Bio-Rad). Protein samples were stored at -80°C. Before 2-dimensional electrophoresis (2-DE) was performed, the protein samples were purified using the Readyprep 2-D cleanup kit (Bio-Rad) according to manufacturer instructions.

Clinical data of the samples

Detailed clinical and pathological data from the health care information center were reviewed. None of the patients had received treatment prior to endoscopy examination. Of the 21 patients, 12 were men and 9 were women; the mean age at the time of the operations was 60.9 years (range: 43-74 years; Table 1). No patient suffered CAG with other concurrent gastric diseases. All CAG tissue samples had definite histological diagnoses: acute and chronic mucosal inflammation (N = 3), acute and chronic mucosal inflammation with mucosa or gland atrophy (N = 7), chronic mucosal inflammation with gastric gland atrophy (N = 7), acute and chronic mucosal inflammation with lymphocytic infiltration (N = 3), and chronic mucosal inflammation. No sample showed low-to-moderate dysplasia or intestinal metaplasia.

Two-dimensional gel electrophoresis

Individual paired samples of normal gastric mucosa and CAG were analyzed by 2-DE as described by Xing et al. (15). Briefly, a 24-cm linear gradient, pH 5-8, ready strip (Bio-Rad) was rehydrated overnight at 16°C with 200 µg protein in 500 µL rehydration buffer (7 M urea, 2 M thiourea, 4% CHAPS, 65 mM DTT, and 0.2% Bio-Lyte). Isoelectric focusing (IEF) was performed using the PROTEAN IEF Cell system (Bio-Rad). After IEF, the immobilized pH gradient strip was immediately equilibrated for 15 min in equilibration buffer I (6 M urea, 2% sodium dodecyl sulfate (SDS), 0.375 M Tris-HCl, pH 8.8, 20% glycerol, and 2% DTT) and then for 15 min in equilibration buffer II (6 M urea, 2% SDS, 0.375 M Tris-HCl, pH 8.8, 20% glycerol, and 2.5% iodoacetamide). SDS-polyacrylamide gel electrophoresis was carried out on 12% SDS-polyacrylamide gels (25 cm x 20.5 cm x 1.0 mm) using the PROTEAN Plus Dodeca Cell system (Bio-Rad) at a constant voltage of 200 V, at 20°C. After electrophoresis, the gels were stained with the Silver Stain Plus Kit (Bio-Rad). The above processes were performed in triplicate for each sample.

Gel imaging and analysis

The silver-stained 2-DE gels were scanned on a GS-800 Calibrated Imaging Densitometer (Bio-Rad) at a resolution of 300 dots per inch. The intensities of protein spots were analyzed with the Amersham Biosciences Imagemaster v 5.0 (USA). The differential protein spots that showed more than 5-fold staining intensity and had the same directional change in at least 9 cases were taken as differentially expressed candidates. The gray values of the protein candidates were analyzed statistically by the nonparametric Wilcoxon test.

Spot cutting and in-gel digestion

To obtain sufficient protein for mass spectrometry, 2-D gels from 21 samples were used for spot cutting. Equal protein masses of each of the 21 samples (normal gastric mucosa and CAG tissue) were pooled, and 300 µg of the mixture was loaded for 2-DE. The differentially expressed protein spots were identified as described in the preceding text. These spots were excised from the gels with the Proteome Works Spot Cutter (Bio-Rad), destained for 20 min in 30 mM potassium ferricyanide/100 mM sodium thiosulfate (1:1, v/v), and washed in Milli-Q water until the gels shrank and were bleached. The pieces of gel were incubated in 0.2 M NH_4HCO_3 for 20 min and dried by lyophilization. Twenty microliters of 20 µg/mL trypsin (Sigma, USA) was added to each gel fragment and the pieces were then incubated at 37°C overnight. The peptides were extracted three times with 50% acetonitrile (ACN) and 0.1% trifluoroacetic acid and dried in a vacuum centrifuge.

Mass spectrometry (MS)

The digests were analyzed using a Bruker Autoflex II TOF/TOF mass spectrometer (Bruker Daltonics Inc., USA) with delayed extraction in which α-cyano-4-hydroxycinnamic acid was exploited as the matrix (in 50% ACN and 0.05% MS). The total 2-µL solution was applied to a target disk and allowed to air dry. Mass-to-charge ratios were measured in a reflector/delayed extraction mode with an accelerating voltage of 20 kV, a grid voltage of 63-65%, positive polarity, and a delay time of 200 nanoseconds. Laser shots at 300 per spectrum were used to acquire the spectra with a range of 800 to 4000 daltons. Trypsin autolysis products

were used for internal mass calibration. Database searching was performed using the Mascot software (http://www.matrixcience.com). The search parameters were the nrNCBI database, human, 10-150 kDa, trypsin (1 missed enzymatic cleavage), and 100-ppm mass tolerance. The best match was the one with the highest score, and a significant match was typically a score of the order of 70 ($P < 0.05$).

Western blot analysis of proteasome activator subunit 1 (PSME1) and ribosomal protein S12 (RPS12)

After the analysis of selected proteins, two differential proteins were confirmed by Western blot analysis in additional samples to validate the 2-DE spot protein content results. Fifteen CAG with individually matched normal mucosa were used for Western blot analysis. Tissue samples were lysed as described above and protein extracts (50 µg) were separated on a 12% SDS-polyacrylamide gel. Proteins were then transferred to a poly-vinylidene difluoride membrane (Bio-Rad). After blocking, the membranes were incubated with a PSME1 goat polyclonal antibody (1:1000 dilution; GenWay Biotech, Inc., USA) and a polyclonal rabbit anti-RPS12 antibody (1:1000 dilution; Sigma-Aldrich, USA). Subsequently the membranes were incubated with anti-goat horseradish peroxidase and anti-rabbit IgG horseradish peroxidase (Abcam, UK), respectively. The specific proteins were visualized with a chemiluminescent reagent (Pierce Biotechnology, USA). As a control for equal protein loading, blots were restained using antiactin antibody (1:4000 dilution; Santa Cruz Biotechnology, USA). The band intensity was analyzed with the PDQuest software ver7.1. The amount of relative expression was calculated as the intensity ratio of RPS12 or PSME1 to that of actin. The association between categorical data was analyzed by the nonparametric Wilcoxon test or the Friedman test, when appropriate, using the SPSS11.0 software package. The level of significance was established at 0.05 (two-tailed).

RT-PCR of PSME1 and RPS12

The total RNAs of additional tissue samples were extracted by homogenization in Trizol (Invitrogen, USA) to validate the 2-DE results and cDNA synthesis was performed in a 20-µL reverse transcription reaction mixture including 5 µg RNA. Amplification of PSME1, RPS12 and β2-MG acting as internal control was then carried out in a DNA thermal cycler (Perkin Elmer, USA) using equal cDNA as template. PCR products were separated by 1.5% agarose gel electrophoresis, scanned and analyzed with the image master VDS system (Pharmacia, USA).

Preliminary functional analysis of PSME1 and RPS12

To understand the roles of PSME1 and RPS12 in CAG, they were imported into Pathway Studio (USA), and an interaction map was generated and visualized with information from the Ensembl database, the Pfam protein families database, Prosite database, GNF GeneAtlas database, and PDB database. Each node represents either a protein entity or a control mechanism of the interaction.

According to the visualized interaction map established by the Pathway Studio, the key pathways including PSME1, RPS12 and other proteins were shown. Furthermore, some preliminary molecular mechanisms underlying CAG were analyzed based on these key pathways.

Results

Differential protein expression of CAG

The 2-DE protein patterns were studied in 21 patients with CAG and individually matched normal mucosa tissue. About 2100 proteins were detected on each gel. The proteins expressed in CAG tissue were compared to those in matched normal tissue. The protein spots that showed 5-fold greater differential expression in at least 9 cases were considered to be differentially expressed candidates (Figure 1A and B). In this study, 18 significantly different candidate protein spots were found. Eight proteins were up-regulated and 10 down-regulated in CAG compared to the same proteins in individually matched normal gastric mucosa. The quantities of all detected spots were analyzed statistically by the nonparametric Wilcoxon test. We then analyzed these candidate spots by MS and identified a total of 15 proteins (Figure 1C and Table 2). The Mascot scores for the protein identified by Bruker Autoflex II TOF/TOF, and other parameters are given in Table 2. We failed to detect 3 protein spots. There might be several reasons for this result, such as lower abundance, some errors in the operation, lower reliability of the MS results, and some characteristics of these proteins. More work will be done on the 3 protein spots in a further study.

Validation of PSME1 and RPS12 by RT-PCR

Using semiquantitative RT-PCR, a 432-bp fragment of PSME1, a 387-bp fragment of RPS12 and an 876-bp control fragment of β2-MG were amplified (Figure 2). The mean ratios of the intensity of the PSME1 band normalized to the control band were 0.23 ± 0.06 and 1.34 ± 0.31 in 15 CAG and normal mucosa tissues, respectively. The P value was lower than 0.05 when the ratios of the two groups were analyzed by the Student *t*-test (Figure 2A). The results of RPS12 were 1.28 ± 0.15 and 0.36 ± 0.09 in 15 CAG and normal mucosa tissues, respectively ($P < 0.05$; Figure 2B). These results suggest that the difference of PSME1 and RPS12 in CAG and normal mucosa tissues can be obvious at the mRNA level.

Validation of PSME1 and RPS12 by Western blot

The two novel candidate proteins, PSME1 and RPS12, were studied further among the differentially expressed proteins. Their expression profiles in CAG have not been reported previously. Western blot analysis showed that RPS12 was significantly up-regulated in CAG tissue (mean

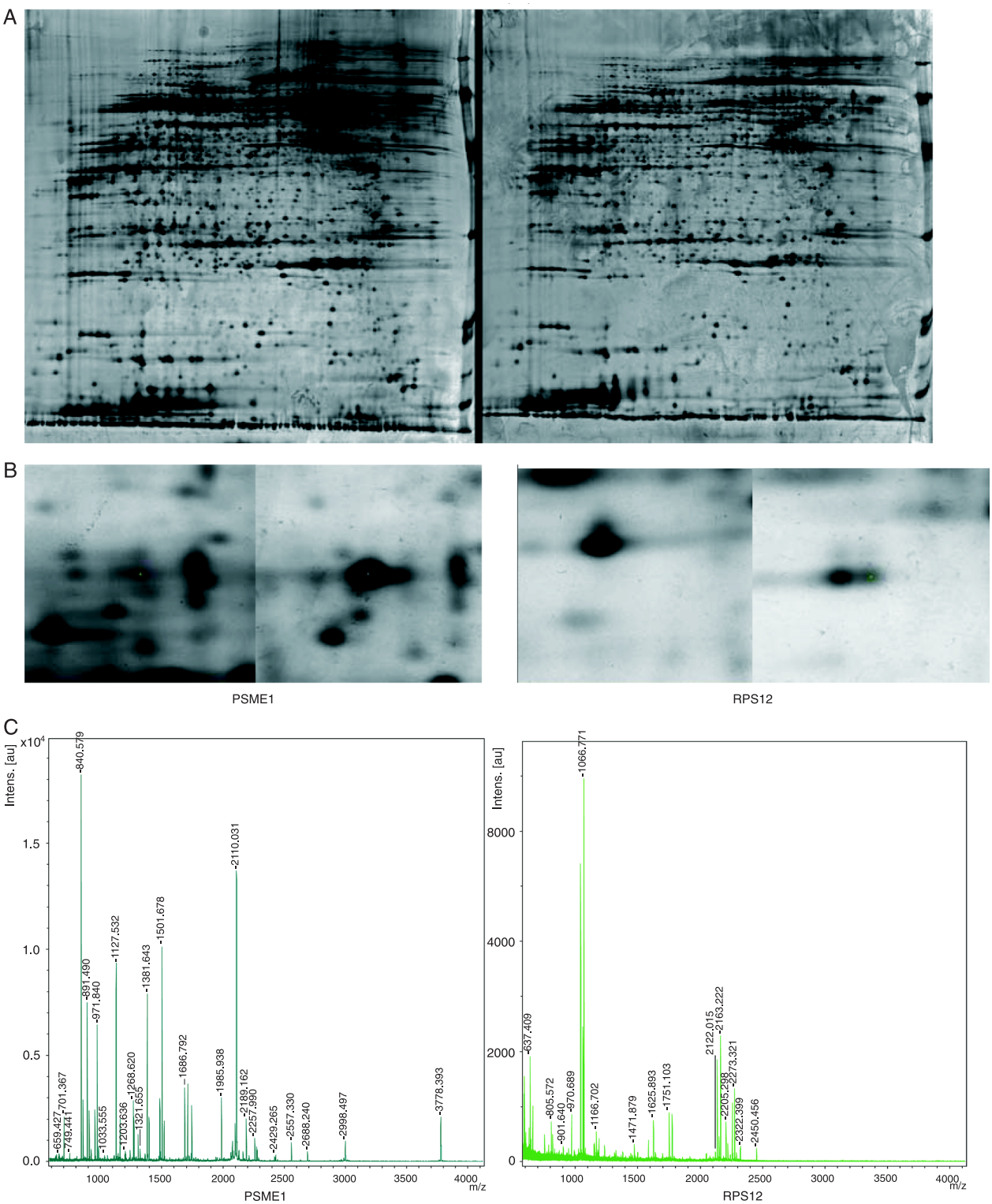

Figure 1. Detection and analysis of differentially expressed proteins in chronic atrophic gastritis (CAG). *A*, Representative 2-DE images of matched CAG and normal gastric mucosa tissue. The proteins expressed in CAG tissue were compared with those expressed in matched normal tissue. Fifteen spots were identified by mass spectrometry in 18 differentially expressed protein spots (Table 2). *B*, Magnified regions of the 2-DE gel of down-regulated PSME1 (left) and up-regulated RPS12 (right) in CAG tissue when compared with normal tissue. *C*, Analysis of the depicted peptide spectrum resulted in the identification of PSME1 (left) and RPS12 (right).

Table 2. Differentially expressed proteins in chronic atrophic gastritis (CAG).

ID No.	Protein identified	Gene identified	Accession No.	Mass (Da)/pI	Cover rate (%)	Mascot scores	Relative intensity (mean ± SD)	General function/comments
Up-regulated proteins								
1	C-C chemokine receptor type 10	CCR10	P46092	38416.4/5.6	42	158	42.8 ± 6.6 5.5 ± 0.6	Receptor for chemokines SCYA27 and SCYA28. Subsequently transduces a signal by increasing the intracellular calcium ion level and stimulates chemotaxis in a pre-B cell line.
2	DNA repair protein RAD51 homolog 2	RAD51L1	O15315	42196.6/6.2	39	201	25.6 ± 3.1 4.2 ± 0.6	Involved in the homologous recombination repair (HRR) pathway of double-stranded DNA breaks arising during DNA replication or induced by DNA-damaging agents.
3	Serine/threonine-protein kinase 19	STK19	P49842	40916.1/4.67	56	106	72.0 ± 12.5 14.3 ± 3.3	Seems to be a protein kinase. *In vitro* it can phosphorylate casein-alpha on serine and threonine residues and histones on serine residues.
4	Hsp90 co-chaperone Cdc37	CDC37	Q16543	44468.4/7.2	47	139	54.3 ± 6.5 8.7 ± 1.4	Co-chaperone that binds to numerous kinases and promotes their interaction with the Hsp90 complex.
5	40S ribosomal protein S12	RPS12	P25398	14515/5.9	64	234	33.7 ± 5.7 6.1 ± 1.4	Belongs to the ribosomal protein S12e family.
6	Protein FAM3C	FAM3C	Q92520	24680.2/6.5	73	231	52.7 ± 4.6 3.8 ± 0.8	Belongs to the FAM3 family.
Down-regulated proteins								
7	Proteasome activator complex subunit 1	PSME1	Q06323	38966.2/7.6	67	173	14.9 ± 5.3 74.2 ± 11.6	Implicated in immuno-proteasome assembly and required for efficient antigen processing.
8	BRCA2 and CDKN1A interacting protein	BCCIP	Q9P287	35979.6/5.8	42	149	5.5 ± 0.8 33.7 ± 8.4	May promote cell cycle arrest by enhancing the inhibition of CDK2 activity by CDKN1A.
9	BTG1 protein	BTG1	P62324	19209.7/6.6	49	204	11.8 ± 1.9 57.2 ± 4.2	Anti-proliferative protein. Its expression is associated with the early G1 phase of the cell cycle.
10	Ubiquitin carboxyl terminal hydrolase isozyme L5	UCHL5	Q9Y5K5	37607.4/8.1	63	224	6.1 ± 1.3 52.8 ± 13.2	Deubiquitinating enzyme associated with the proteasome.
11	Succinate dehydrogenase [ubiquinone] iron-sulfur subunit, mitochondrial	SDHB	P21912	31636/6.2	50	161	13.9 ± 3.1 75.3 ± 12.8	Involved in complex II of the mitochondrial electron transport chain.
12	Caspase-7	CASP7	P55210	34277.1 /8.2	39	211	4.9 ± 1.3 39.2 ± 5.4	Involved in the activation cascade of caspases responsible for apoptosis execution.
13	Apoptosis-associated speck-like protein containing a CARD	PYCARD	Q9ULZ3	21627.7 /4.6	61	147	2.3 ± 0.3 14.8 ± 2.9	Promotes caspase-mediated apoptosis.
14	Histone deacetylase 3	HDAC3	O15379	48848.4 /5.6	68	230	12.4 ± 3.4 74.3 ± 13.1	Responsible for the deacetylation of lysine residues on the N-terminal part of the core histones.
15	Protein fem-1 homolog B	FEM1B	Q9UK73	70264.2/8.3	54	163	4.6 ± 1.1 34.4 ± 7.5	Component of an E3 ubiquitin-protein ligase complex, in which it may act as a substrate recognition subunit.

Mascot scores are the sum of values stained for peptides recovered from that protein. The relative intensity data are reported for CAG (top) and normal (bottom) tissues.

± SD: 0.59 ± 0.08) but not in normal gastric mucosa tissue (mean ± SD: 0.22 ± 0.06; Figure 3B). Compared to normal mucosa (mean ± SD: 0.66 ± 0.10), PSME1 was significantly down-regulated in CAG tissue (mean ± SD: 0.12 ± 0.03) ($P < 0.05$, Student *t*-test or Friedman test) (Figure 3A).

Preliminary functional analysis

PSME1 and RPS12 were imported into Pathway Studio to build an interaction network. The connectivity of PSME1 and RPS12 was 64 and 38, respectively. The average connectivity of the proteins identified was about 43. Our results showed that PBP, RAF1, Braf, MAPK1, and MAP2K1 were hot points with more connectivity. Based on the molecular network, we concluded that the PBP-RAF/MAPK pathway and NF-kappaB (NF-κB) signaling pathway could be the cores of the whole network. Cancer and other phenotypes interested in downstream such as inflammation, necrosis and hyperplasia were linked to the two pathways (Figure 4).

Discussion

It is well known that chronic CAG plays a crucial role in the development of gastric cancer, which is one of the most common causes of cancer deaths globally. *H. pylori* has been thought to be the major trigger of CAG (16). But there are still many CAG patients without *H. pylori* infection and

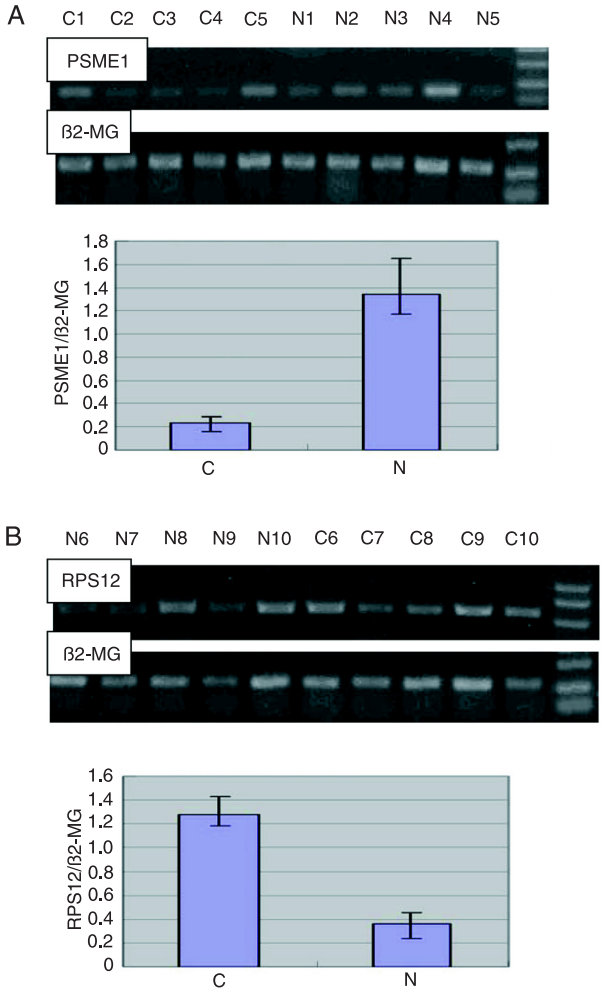

Figure 2. RT-PCR analysis of PSME1 and RPS12. *A*, Down-regulation of PSME1 in chronic atrophic gastritis (CAG) (C) tissue. RT-PCR assays were performed to confirm the differential expression of the PSME1 protein between CAG and normal (N) gastric mucosa. Amplification of PSME1 and of β2-MG acting as internal control was then carried out in a DNA thermal cycler. The bands were quantified by densitometry scanning. The relative quantification was calculated as the ratio of PSME1 expression to β2-MG expression as shown in the bar graph. *B*, Up-regulation of RPS12 in CAG (C) tissue compared to normal (N) mucosa. The same experimental process was performed. The relative quantification was calculated as the ratio of RPS12 expression to β2-MG expression as also shown in the bar graph.

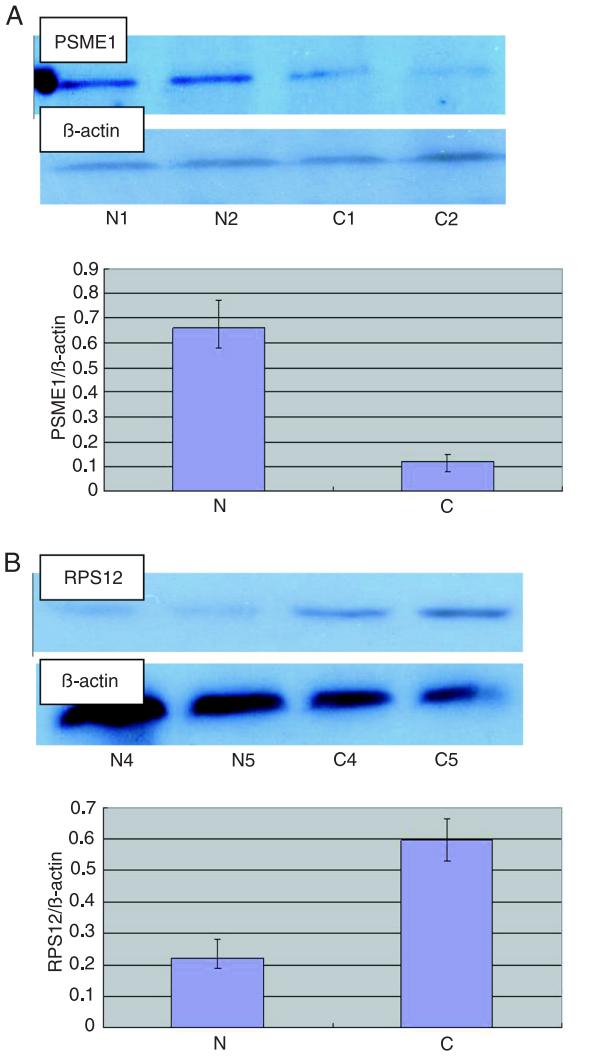

Figure 3. Western blot analysis of PSME1 and RPS12. *A*, Down-regulation of PSME1 in chronic atrophic gastritis (CAG) (C) tissue. Western blot assays were performed to demonstrate the differential expression of the PSME1 protein between CAG and normal (N) gastric mucosa. The specific proteins were visualized with a chemiluminescent reagent. As a control for equal protein loading, blots were restained with antiactin antibody. Immunosignals were quantified by densitometry scanning. The relative quantification was calculated as the ratio of PSME1 to actin as shown in the bar graph. *B*, Up-regulation of RPS12 in CAG (C) tissue compared to normal (N) mucosa. The same experimental process was performed. The relative quantification was calculated as the ratio of RPS12 to actin as also shown in the bar graph.

most of the previous studies were clinical investigations in which very few genes and proteins were connected with the disease. Thus, we still do not clearly know what occurs in the change from morphologically normal mucosa to CAG. Meanwhile, the patients could face a higher risk of gastric cancer. Thus, it is important to investigate the molecular mechanism underlying CAG. Proteomic methods will help us to understand the early stages in the progress of CAG for the prevention and treatment of gastric cancer. In this study, we used the common 2-DE approach coupled with MS to study the differentially expressed proteins in individually matched cases of normal mucosa and CAG lesion and

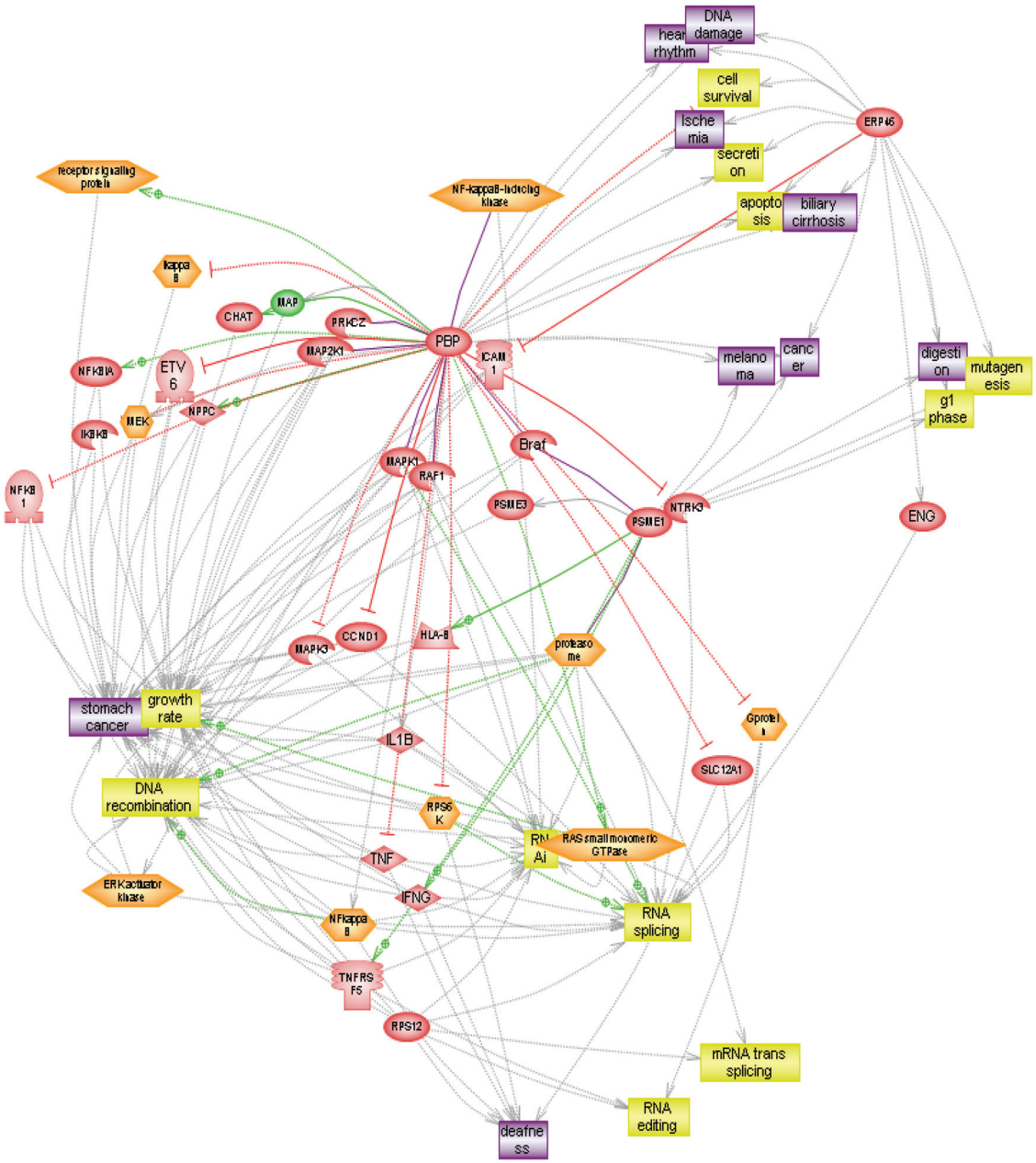

Figure 4. Biological interaction networking of PSME1 and RPS12 in chronic atrophic gastritis (CAG). PSME1 and RPS12 were imported into Pathway Studio (USA) and an interaction map was generated with information from the Ensembl database, the Pfam protein families database, Prosite database, GNF GeneAtlas database, and PDB database. Each node represents either a protein or a control mechanism of the interaction. The NF-κB and PBP-RAF/MAPK signaling pathways could be major molecular interaction pathways. The compendious molecular interaction pathway, which linked PSME1, RPS12 and PBP, could impact on some cell functions such as cell proliferation and apoptosis, and the cell cycle could then promote the formation of CAG.

confirmed the differential expression of PSME1 and RPS12 by Western blot and RT-PCR analysis.

Eighteen differentially expressed proteins were identified in CAG in the study, and none of them (Table 2) had been reported in previous studies on this disease. We used a cut-off of 5-fold in the research. This high cut-off may have

missed some potentially important changes, although it could minimize the possibility of individual difference and ensure the fidelity of the change. In the current study, we only found 18 differentially expressed proteins between CAG and normal mucosa in the fluorescence difference gel electrophoresis study. But we believe that some major molecular mechanisms underlying the disease should be implicated. A concept of cancer biology is that tumors arise and grow from some precancerous lesion as a result of the multiple changes of some genes or proteins, which could influence some cell functions via different molecular biological pathways. Thus, it would be very important to determine these molecular changes and their functional pathways. There may be not too many changes in the expressions of proteins in the original step towards gastric cancer, namely CAG, and therefore only 18 differentially expressed proteins were found. There were also some methodological discrepancies in the processes of our proteomic study, including sample collection, the separation and identification of proteins and analysis of the results. Some low-abundance protein spots could not be displayed clearly and these proteins should be further analyzed by a more advanced method.

In the present study, we confirmed that PSME1 expression was significantly down-regulated in CAG tissue compared to normal mucosa. The same finding about this protein has been reported in previous studies (17-20). An alternative name of PSME1 is PA28 alpha that encodes the alpha subunit of the 11S regulator. This 11S regulator is an important component of the 26S proteasome, which is composed of 2 complexes, a 20S core, and a 19S or 11S regulator. The proteasome is expressed throughout eukaryotic cells and disintegrates proteins in a ubiquitin-dependent pathway in which many products of oncogenes and anti-oncogenes are decomposed. The other essential function of the proteasome is the processing of class I major histocompatibility complex peptides, namely immunoproteasome. The results of previous studies (17-20) have revealed that the noticeable function of PSME1 was immunoregulation, which, to some extent, could enhance anticancer immunological reaction. The relationship between PSME1 and some cancers has been reported recently. Zhang et al. (21) found that PSME1 was down-regulated in HBV-infected hepatocellular carcinoma in a comparative proteomics research to analyze the differential proteome of tumor and adjacent non-tumor tissues, and thought that PSME1 could play an important role in the onset of hepatocarcinogenesis. Miyagi et al. (22) confirmed that the expression of PSME1 was impaired in some human colon cancer cell lines, and they thought that this change could be involved in the loss of HLA class I expression in human colon cancer cells. Lemaire et al. (23) reported that PSME1 could be regarded as a potential biomarker of ovary cancer because of its outstanding differential expression between ovary cancer and normal tissue. Collectively, these studies suggest that the PSME1 gene could be involved in cancer initiation and progression because of impaired immunoprotection. Our results confirmed that PSME1 expression is down-regulated in CAG compared to normal mucosa. We postulated that this down-regulation of PSME1 might denote a step of the potential cancerous transformation of the gastric mucosa due to weakened immunological function.

RPS12 was significantly up-regulated in CAG tissue although its expression remained unchanged in normal mucosa. The RPS12 gene encodes a ribosomal protein, which is an important component of the 40S subunit of ribosomes. Ribosomes are highly conserved large ribonucleoprotein particles consisting of a large 60S subunit and a small 40S subunit that perform protein synthesis. There are many different ribosomal proteins (r-proteins), which are encoded by different genes scattered about the genome. The function of ribosomes is very complex, with different steps occurring in different parts of the cell. Separate ribosomal subunits are then transported from the nucleolus to the cytoplasm where they assemble into mature ribosomes before functioning in translation. In this process, r-proteins such as the protein product of RPS12 form the ribosomal subunits and perform the functional roles of identification, integration, and transport. Thus, the change in the expression of an r-protein could result in up-regulation or down-regulation of newly synthesized proteins. The change in the expression of RPS12 could influence the expression of some proteins. On the other hand, because there are many r-proteins and their roles may overlap, the changes in expression of a single ribosomal protein could have a very limited impact on global gene expression. Thus, the up-regulation of RPS12 could result in the changes in the expression of some proteins but the number of these changed proteins could be limited. The results of some previous investigations have revealed that this gene could be related to some human cancer. Cheng et al. (24), using RT-PCR differential display and cDNA microarray methods, found that the expression of RPS12 may be up-regulated in the adjacent histopathologically "normal" cervical squamous epithelial tissue from cervical cancer patients. Thus, they thought that RPS12 could be a potential biomarker for an early diagnosis of human cervical cancer. Deng et al. (25), using comparative proteome analysis of breast cancer and adjacent normal breast tissues, found that the expression of RPS12 could be changed in breast cancer and be involved in the pathological process of this disease. Sun et al. (26), using suppression subtractive hybridization methods, revealed that the expression of RPS12 was higher in early and advanced gastric cancer and in lymph node metastases than in normal mucosa. Based on these reports, we think that the RPS12 gene could be a tumor-enhancing gene, but the detailed biological roles of RPS12 in CAG and gastric cancer remain to be elucidated. The up-regulation of RPS12 in CAG suggests that this disease may be related to gastric cancer and RPS12 may play a crucial role in the

initiation of cancerization.

Our bioinformatics results suggested that the PBP-RAF/MAPK and NF-κB pathways could be the crucial signal transduction pathways of the molecular change in CAG. The NF-κB and PBP-RAF/MAPK signaling pathways regulate the growth of many tumors or inflammation, suggesting co-operation between these two pathways in the regulation of cell proliferation and apoptosis in CAG. It is well known that *H. pylori* is the cause of many gastric diseases, including CAG. The results of some investigations on *H. pylori* have revealed that the PBP-RAF/MAPK and NF-κB pathways could be the crucial mechanism of the pathopoiesis of *H. pylori*. Fox and Wang (27), Shibata et al. (28), and Lee et al. (29) have confirmed that the induction of cytokines and chemokines and growth-related genes by *H. pylori* is mediated by the PBP-RAF/MAPK and NF-κB signaling pathways. In our molecular interaction network of CAG, the changes of PSME1 or RPS12 and the impact on the NF-κB and PBP-RAF/MAPK signaling pathways could be analogous to the reaction to *H. pylori* infection. But the patients in our study were not infected with *H. pylori*, and therefore, according to previous reports, we supposed that CAG without *H. pylori* infection could involve a pathogenesis similar to that of CAG with *H. pylori* infection, in which a series of molecular interactions were induced by an immunological reaction against *H. pylori* infection. But in CAG without *H. pylori* infection, the initiating agent could not be *H. pylori* but other infectious agents or molecules.

Of 16 other differentially expressed proteins, 7 were up-regulated and 9 down-regulated in CAG when compared to the same proteins in individually matched normal gastric mucosa. Some of the up-regulated proteins are mainly involved in inflammation, such as CCR10 and CDC37 (30,31), with effects on the release of inflammatory cytokines or angiogenesis. The RAD51L1 protein may be involved in the homologous recombination repair pathway of double-stranded DNA in cells (32) and STK19 may be involved in transcriptional regulation (33). FAM3C is a member of the family with sequence similarity 3 (FAM3) and encodes a secreted protein with a GG domain and may be up-regulated in some cancer cells like other members of this family (34). Many of the down-regulated proteins are involved in cell cycle regulation or in the promotion of apoptosis. For example, BCCIP and BTG1 may regulate the cell cycle and promote cell cycle arrest (35). CASP7 and PYCARD proteins are involved in caspase-mediated apoptosis (36). Other down-regulated proteins may inhibit cell growth and proliferation and may be considered to be potential tumor suppressor genes, such as HDAC3 (37). In summary, many up-regulated proteins could participate in the regulation of transcription, in DNA repair or proliferation, whereas many down-regulated proteins could inhibit cell division and promote apoptosis.

In short, our study showed a differential protein expression profile of CAG compared to matched normal mucosa. The candidate proteins confirm the conclusion that CAG is one of the major precursor diseases of gastric cancer; thus, more effective treatment should be applied to the disease.

Acknowledgments

We thank the Beijing Proteomic Research Center, the Institute of Biochemistry and Cell Biology, the Fourth Military Medical University.

References

1. Weck MN, Brenner H. Prevalence of chronic atrophic gastritis in different parts of the world. *Cancer Epidemiol Biomarkers Prev* 2006; 15: 1083-1094.
2. Ferlay J, Bray F, Pisani P, Parkin DM. *GLOBOCAN 2002: Cancer incidence, mortality and prevalence worldwide. IARC CancerBase No. 5, version 2.0*. Lyon: IARC Press; 2004.
3. Tsugane S, Kabuto M, Imai H, Gey F, Tei Y, Hanaoka T, et al. *Helicobacter pylori*, dietary factors, and atrophic gastritis in five Japanese populations with different gastric cancer mortality. *Cancer Causes Control* 1993; 4: 297-305.
4. Fukao A, Komatsu S, Tsubono Y, Hisamichi S, Ohori H, Kizawa T, et al. *Helicobacter pylori* infection and chronic atrophic gastritis among Japanese blood donors: a cross-sectional study. *Cancer Causes Control* 1993; 4: 307-312.
5. Tatematsu M, Yamamoto M, Shimizu N, Yoshikawa A, Fukami H, Kaminishi M, et al. Induction of glandular stomach cancers in *Helicobacter pylori*-sensitive Mongolian gerbils treated with N-methyl-N-nitrosourea and N-methyl-N'-nitro-N-nitrosoguanidine in drinking water. *Jpn J Cancer Res* 1998; 89: 97-104.
6. Sugiyama A, Maruta F, Ikeno T, Ishida K, Kawasaki S, Katsuyama T, et al. *Helicobacter pylori* infection enhances N-methyl-N-nitrosourea-induced stomach carcinogenesis in the Mongolian gerbil. *Cancer Res* 1998; 58: 2067-2069.
7. Shimizu N, Inada K, Nakanishi H, Tsukamoto T, Ikehara Y, Kaminishi M, et al. *Helicobacter pylori* infection enhances glandular stomach carcinogenesis in Mongolian gerbils treated with chemical carcinogens. *Carcinogenesis* 1999; 20: 669-676.
8. Parkin DM, Pisani P, Ferlay J. Global cancer statistics. *CA Cancer J Clin* 1999; 49: 33-64.
9. Correa P. A human model of gastric carcinogenesis. *Cancer Res* 1988; 48: 3554-3560.
10. Correa P. The epidemiology of gastric cancer. *World J Surg* 1991; 15: 228-234.
11. Correa P. Human gastric carcinogenesis: a multistep and multifactorial process - First American Cancer Society Award Lecture on Cancer Epidemiology and Prevention. *Cancer Res* 1992; 52: 6735-6740.
12. Sipponen P, Jarvi O, Kekki M, Siurala M. Decreased incidences of intestinal and diffuse types of gastric carcinoma

in Finland during a 20-year period. *Scand J Gastroenterol* 1987; 22: 865-871.
13. Rios-Castellanos E, Sitas F, Shepherd NA, Jewell DP. Changing pattern of gastric cancer in Oxfordshire. *Gut* 1992; 33: 1312-1317.
14. Wulfkuhle JD, Liotta LA, Petricoin EF. Proteomic applications for the early detection of cancer. *Nat Rev Cancer* 2003; 3: 267-275.
15. Xing X, Lai M, Gartner W, Xu E, Huang Q, Li H, et al. Identification of differentially expressed proteins in colorectal cancer by proteomics: down-regulation of secretagogin. *Proteomics* 2006; 6: 2916-2923.
16. Peek RM Jr, Blaser MJ. *Helicobacter pylori* and gastrointestinal tract adenocarcinomas. *Nat Rev Cancer* 2002; 2: 28-37.
17. Obata C, Zhang M, Moroi Y, Hisaeda H, Tanaka K, Murata S, et al. Formalin-fixed tumor cells effectively induce antitumor immunity both in prophylactic and therapeutic conditions. *J Dermatol Sci* 2004; 34: 209-219.
18. Sun Y, Sijts AJ, Song M, Janek K, Nussbaum AK, Kral S, et al. Expression of the proteasome activator PA28 rescues the presentation of a cytotoxic T lymphocyte epitope on melanoma cells. *Cancer Res* 2002; 62: 2875-2882.
19. Kuckelkorn U, Ferreira EA, Drung I, Liewer U, Kloetzel PM, Theobald M. The effect of the interferon-gamma-inducible processing machinery on the generation of a naturally tumor-associated human cytotoxic T lymphocyte epitope within a wild-type and mutant p53 sequence context. *Eur J Immunol* 2002; 32: 1368-1375.
20. Sijts A, Sun Y, Janek K, Kral S, Paschen A, Schadendorf D, et al. The role of the proteasome activator PA28 in MHC class I antigen processing. *Mol Immunol* 2002; 39: 165-169.
21. Zhang D, Lim SG, Koay ES. Proteomic identification of down-regulation of oncoprotein DJ-1 and proteasome activator subunit 1 in hepatitis B virus-infected well-differentiated hepatocellular carcinoma. *Int J Oncol* 2007; 31: 577-584.
22. Miyagi T, Tatsumi T, Takehara T, Kanto T, Kuzushita N, Sugimoto Y, et al. Impaired expression of proteasome subunits and human leukocyte antigens class I in human colon cancer cells. *J Gastroenterol Hepatol* 2003; 18: 32-40.
23. Lemaire R, Menguellet SA, Stauber J, Marchaudon V, Lucot JP, Collinet P, et al. Specific MALDI imaging and profiling for biomarker hunting and validation: fragment of the 11S proteasome activator complex, Reg alpha fragment, is a new potential ovary cancer biomarker. *J Proteome Res* 2007; 6: 4127-4134.
24. Cheng Q, Lau WM, Tay SK, Chew SH, Ho TH, Hui KM. Identification and characterization of genes involved in the carcinogenesis of human squamous cell cervical carcinoma. *Int J Cancer* 2002; 98: 419-426.
25. Deng SS, Xing TY, Zhou HY, Xiong RH, Lu YG, Wen B, et al. Comparative proteome analysis of breast cancer and adjacent normal breast tissues in human. *Genomics Proteomics Bioinformatics* 2006; 4: 165-172.
26. Sun XJ, Hao DM, Zheng ZH, Fu H, Xu HM, Wang MX, et al. [Screening and analysis of associated genes in the carcinogenesis and progression of gastric cancer]. *Zhonghua Yi Xue Yi Chuan Xue Za Zhi* 2005; 22: 31-34.
27. Fox JG, Wang TC. *Helicobacter pylori* infection: pathogenesis. *Curr Opin Gastroenterol* 2002; 18: 15-25.
28. Shibata W, Hirata Y, Ogura K, Omata M, Maeda S. [NF-kappaB and MAPK-signaling pathways contribute to the gene expression and host response induced by *Helicobacter pylori* infection]. *Nihon Rinsho* 2005; 63 (Suppl 11): 132-137.
29. Lee JS, Kim HS, Hahm KB, Sohn MW, Yoo M, Johnson JA, et al. Inhibitory effects of 7-carboxymethyloxy-3',4',5-trimethoxyflavone (DA-6034) on *Helicobacter pylori*-induced NF-kappa B activation and iNOS expression in AGS cells. *Ann N Y Acad Sci* 2007; 1095: 527-535.
30. Marchese A, Docherty JM, Nguyen T, Heiber M, Cheng R, Heng HH, et al. Cloning of human genes encoding novel G protein-coupled receptors. *Genomics* 1994; 23: 609-618.
31. Dai K, Kobayashi R, Beach D. Physical interaction of mammalian CDC37 with CDK4. *J Biol Chem* 1996; 271: 22030-22034.
32. Rice MC, Smith ST, Bullrich F, Havre P, Kmiec EB. Isolation of human and mouse genes based on homology to REC2, a recombinational repair gene from the fungus *Ustilago maydis*. *Proc Natl Acad Sci U S A* 1997; 94: 7417-7422.
33. Sargent CA, Anderson MJ, Hsieh SL, Kendall E, Gomez-Escobar N, Campbell RD. Characterisation of the novel gene G11 lying adjacent to the complement C4A gene in the human major histocompatibility complex. *Hum Mol Genet* 1994; 3: 481-488.
34. Zhu Y, Xu G, Patel A, McLaughlin MM, Silverman C, Knecht K, et al. Cloning, expression, and initial characterization of a novel cytokine-like gene family. *Genomics* 2002; 80: 144-150.
35. Liu J, Yuan Y, Huan J, Shen Z. Inhibition of breast and brain cancer cell growth by BCCIPalpha, an evolutionarily conserved nuclear protein that interacts with BRCA2. *Oncogene* 2001; 20: 336-345.
36. Entrez Gene: CASP7 caspase 7, apoptosis-related cysteine peptidase. Gene ID: 840.
37. Emiliani S, Fischle W, Van Lint C, Al-Abed Y, Verdin E. Characterization of a human RPD3 ortholog, HDAC3. *Proc Natl Acad Sci U S A* 1998; 95: 2795-2800.